

# Nanoporous Networks of Si-, Al-, P-Oxygen Tetrahedra with Encapsulated Dyes as New Composite Materials

D. Wöhrle,<sup>\*1</sup> G. Schulz-Ekloff,<sup>1</sup> C. Bräuchle,<sup>2</sup> F. Laeri<sup>3</sup>

**Summary:** Microporous and mesoporous molecular sieves like zeolite faujasites,  $\text{AlPO}_4\text{-5}$  and  $\text{Si-MCM-41}$  are obtained by polycondensation of oxygen containing tetrahedra of the metal aluminium, the semimetal silicon and the non-metal phosphorus by conventional or microwave-assisted hydrothermal synthesis. The encapsulation of dyes after different methods is described. Monomolecular distribution of dyes in the framework of the hosts is obtained. The encapsulated dyes show high absorption and fluorescence intensities which is interesting for photochromic switches, optical sensors and lasing. The location of a dye is identified after single molecule spectroscopy.

**Keywords:** dyes; molecular sieves; nanoporous; optical properties

## Introduction

Inorganic molecular sieves contain channels and cavities of molecular dimensions (microporous materials with diameter of  $\sim 0.35\text{--}1.5$  nm, mesoporous materials with diameter of  $\sim 1.5\text{--}20$  nm). These nanoporous networks play a major role in material science because of the possibility that physical and chemical properties can be tuned widely, for example, pore diameter, polarity or chemical affinity of the internal surface.<sup>[1]</sup> Inorganic molecular sieves have very high internal surface area (up to more than  $1000\text{ m}^2\text{ g}^{-1}$ ) and therefore high adsorption capacities. Several places for interactions with guest molecules exist. The structural peculiarities of inorganic molecular sieves enable the incorporation of optically active guests often in crystallographically defined positions or highly

organized arrangements.<sup>[2,3]</sup> The monomer encapsulation leads to composite materials with novel properties, which goes far beyond the traditional areas and points out domains of electronic and optical applications.<sup>[2,3]</sup> In the following at first the network formation to get nanoporous systems starting from low molecular metal, semimetal and non-metal precursors is exemplarily pointed out. Then different methods for the encapsulation of organic dyes and properties of the composite materials are described. All steps for the syntheses of molecular sieves and the different methods of dyes encapsulations must be carefully controlled by X-ray diffraction, nitrogen sorption, FTIR and UV/Vis reflectance spectroscopy.

## The Hosts Inorganic Molecular Sieves

Zeolites are aluminosilicates with the metal aluminium and the semimetal silicon of the composition in the case of Faujasites of  $x/n\text{M}^n[(\text{AlO}_2)_x(\text{SiO}_2)_y]_w\text{H}_2\text{O}$  with a negatively-charged lattice.<sup>[4]</sup> They consist of edge-connected  $[\text{Si(IV)O}]$  and  $[\text{Al(III)O}]^-$

<sup>1</sup> Universität Bremen, Institut für Organische und Makromolekulare Chemie, P.O. Box 330440, 28334 Bremen, Germany

E-mail: woehrle@chemie.uni-bremen.de

<sup>2</sup> Department of Chemistry and Biochemistry, Universität München, 81377 München, Germany

<sup>3</sup> Institute of Applied Physics, Technische Universität Darmstadt, 64289 Darmstadt, Germany

tetrahedra with charge compensating inorganic cations like  $\text{Na}^+$ . In faujasite zeolites the diameter of the supercage is 1.3 nm with windows of 0.74 nm. The microporous molecular sieve  $\text{AlPO}_4\text{-5}$  of the composition  $n\text{T}[(\text{AlO}_2)(\text{PO}_2)]_w\text{H}_2\text{O}$  ( $\text{T}$  = template) exhibits a hexagonal anisotropic, one dimensional channel structure with a channel diameter of 0.73 nm in the direction of the crystallographic  $c$  axis. The lattice of  $\text{AlPO}_4\text{-5}$  is constructed with the metal aluminium and the non-metal phosphorus by alternating  $[\text{Al(III)O}]^-$  and  $[\text{P(V)O}]^+$  tetrahedra leading to a neutral lattice.<sup>[5]</sup> Finally, the mesoporous silicates of the M41S family like Si-MCM-41 (channel diameter  $\sim 3.1$  nm) with connected  $[\text{Si(IV)O}]$  tetrahedra in the composition  $n\text{D}[\text{SiO}_2]_2w\text{H}_2\text{O}$  ( $\text{D}$  = detergent) are mentioned.<sup>[6]</sup> These silicates are ordered, but not conventionally crystalline, since the pore walls are usually amorphous.

For the synthesis of inorganic molecular sieves mainly methods based on empirical experiences are used because the mechanisms of formation are often not known in detail. The syntheses start from low mole-

cular sources of oxygen containing  $\text{Al(III)}$ ,  $\text{Si(IV)}$  and  $\text{P(V)}$ . Temperature, pressure, pH value (acidic or basic), time of crystallization, concentration of reagents and the presence of a structure directing organic agent are important parameters to be considered in the direction of a specific molecular sieve phase. The formations are polycondensations occurring through the reaction of the precursors. Exemplarily the formations of  $\text{AlPO}_4\text{-5}$  and Si-MCM-41 are mentioned.

Aluminumphosphates like  $\text{AlPO}_4\text{-5}$  are prepared hydrothermal under autogenous pressure in the temperature range of 100–250 °C.<sup>[5,7]</sup> Based on a mixture of  $\text{Al(O)OH}$  or Al alkoxides and phosphoric acid in water a aluminumphosphate gel is formed first, and then in the case of  $\text{AlPO}_4\text{-5}$  the template tri-*n*-propylamine as structure directing agent is added. At first, phosphate ions form in a weakly acidic medium covalent bonds by bridged oxygen with aluminum atoms. Important is then the condensation of these molecular aluminophosphates to one-dimensional polymer chains consisting of four-membered-rings

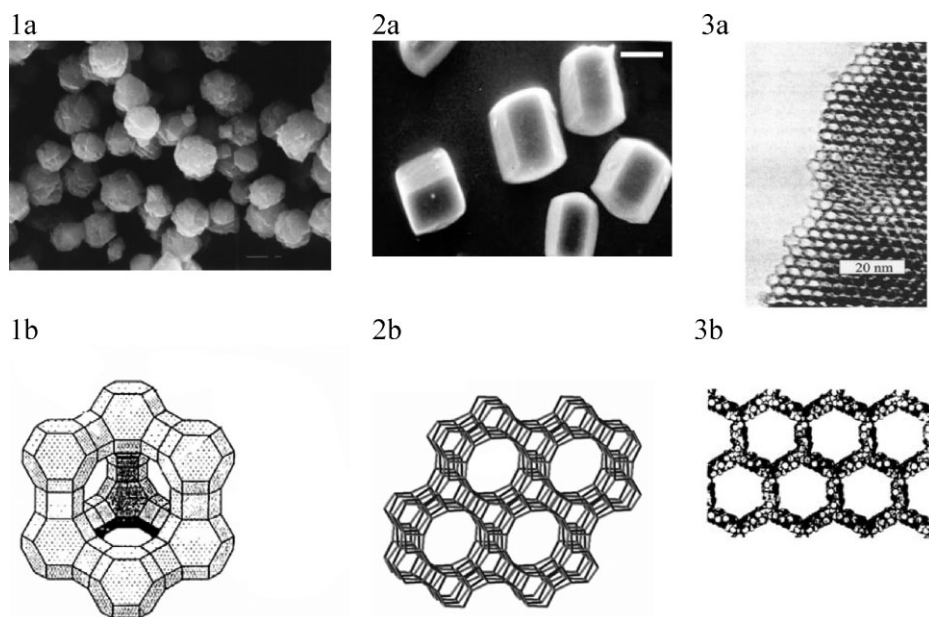


**Figure 1.** Morphologies and molecular structures of zeolite faujasite (1a,b),  $\text{AlPO}_4\text{-5}$  (2a,b) and Si-MCM-41 (3a,b).

of Al(III) centers with the unit  $[\text{AlOO-P}(\text{OH})_2\text{OO}]_n$ .<sup>[8]</sup> The linear chains are meta-stable and can partially hydrolyze to open chain moieties with Al-OH and P-OH groups. In dependence on the structure directing agent and the reaction conditions these precursor chains condense via two-dimensional porous layer structures to three-dimensional microporous solids. The cationic structure directing amines (pH at the beginning is slightly acidic) reduce the electrostatic repulsion between the precursor chains by formation of ionic and/or hydrogen bonds. Crosslinking between the chains results stepwise in a porous structure. The long reaction time of around one day (at  $T \sim 150^\circ\text{C}$ ) can be reduced to several minutes under conditions of the microwave-assisted hydrothermal synthesis as mentioned below.<sup>[7]</sup>

In addition, fundamentals of the procedure for the synthesis of the silicates of the MCM-41 are given. Suitable amounts of a silicate source (e.g. tetraethoxysilane, TEOS), a cationic detergent (e.g. cetyltrimethylammonium chloride, CTAC), tetramethylammonium hydroxide (TMAOH) and water are mixed.<sup>[6]</sup> The mixture is heated for 24 till 144 h up to a temperature of  $\sim 100^\circ\text{C}$ . Under microwave-assisted conditions the reaction time is reduced to  $\sim 15$  min.<sup>[9]</sup> By calcination at  $T \sim 500^\circ\text{C}$  or treatment with solvents the template-free mesoporous silicate can be obtained. The mechanism for the formation of Si-MCM-41 under alkaline is shown schematically in Figure 2. The detergent forms rod-shaped micelles which further organize to a hexagonal liquid phase interacting then at

high pH values with the silicate anion which results in hexagonal arrays of a silicate layer.<sup>[6,10]</sup>

It was pointed out before that under the microwave-assisted conditions compared to the conventional conditions the reaction time is drastically reduced. This can be related to the different heating process using microwave radiation at 2450 MHz. When microwave energy penetrates the gel mixture, a rapid heating occurs because the radiation at 2450 MHz matches the rotation frequency of the water dipoles. It must be pointed out that under these changed reaction conditions the gel composition of the reactants must be changed in order to get pure a pure phase of the molecular sieve.<sup>[7c]</sup> One possibility for the encapsulation of dye molecules is the addition of a dye to the gel mixture of the hydrothermal synthesis as discussed below. Under the conditions of the conventional hydrothermal synthesis with a long reaction time polar dye molecules react more easily and are destroyed. This can be avoided under by the short reaction time of the microwave assisted synthesis. This is shown in Figure 3 for Coumarin 40 added to the gel mixture of the  $\text{AlPO}_4\text{-5}$  synthesis.<sup>[7a]</sup>

The defined cavity/channel diameter, the high internal surface area, the excellent mechanical stability and specific host/guest interactions are important factors for the inclusion of dyes and colored metal complexes. In relation to the optical properties of encapsulated coloured compounds, the transmission for visible light and the optical homogeneity are other important parameters. In the following examples for

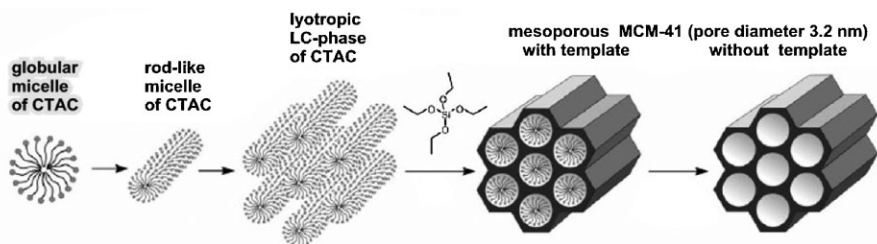


**Figure 2.**  
Si-MCM-41 formation after the LC-template mechanism.

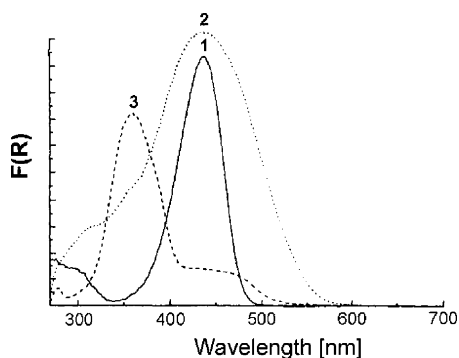


**Figure 3.**

Absorption spectrum of Coumarin 40 **1** in water (1). Reflectance spectra of **1** in  $\text{AlPO}_4\text{-5}$  obtained at  $T = 150^\circ\text{C}$  under microwave conditions after 45 min (2) and by conventional synthesis after 4 h (3).

permanent inclusion of these guests obtained by different methods and the optical properties of the composite materials are given.<sup>[2,3]</sup> The encapsulation of some dyes shown in Figure 4 will be discussed.

### In Situ Syntheses of Dyes in Zeolite Faujasites

The *in situ* synthesis (also called “ship-in-the-bottle” technique) of phthalocyanine metal complexes, azo dyes and spiropyran dyes in faujasites NaY, HY and DAY was in detail described by our group.<sup>[11–13]</sup> Exemplarily, the synthesis of the photochromic spiropyran is discussed. The *in situ*

synthesis enables to include polar dyes and to build-up chromophore molecules with diameters exceeding the window width of the zeolite cages. After their formation the dyes cannot be removed by solvent extraction (size of synthesized spiropyran dye **2**:  $1.4 \times 0.74 \times 0.35 \text{ nm}^3$ ; faujasite diameter of windows 0.74 nm and of supercages 1.3 nm). The developed method for the synthesis of pure organic chromophores in the supercages of faujasites follows the simple scheme  $A + B \rightarrow C$ . In a first step a precursor for the dye has to be fixed by interaction with the zeolite lattice on adsorption sites. For example, a basic precursor A (for the synthesis of **2**: 1,3,3-methyl-2-methylene-indoline) are bound by acid-base interaction with the host (Figure 5). Therefore, HY (acidic  $\text{H}^+$  exchanged faujasite) is preferable compared to NaY ( $\text{Na}^+$  exchanged faujasite) and DAY (partially dealuminated faujasite). After careful cleaning of the molecular sieve from the excess of non-interacting basic precursors, the chromophore synthesis is achieved by diffusing the second educt B (for the synthesis of **2**: 5-nitrosalicylaldehyde) into the porous zeolite structure and subsequent reaction. Whereas the small educt molecules can enter the pore system, the larger size of the formed dye molecules inhibits their diffusion out of the supercages. The *in situ* synthesis of **2** in the faujasite structures NaY, HY or DAY yielded loadings, which can be expressed as percent

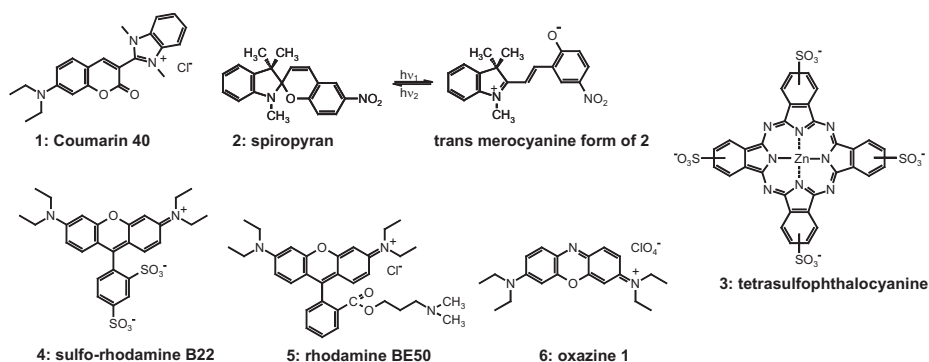


**Figure 4.**

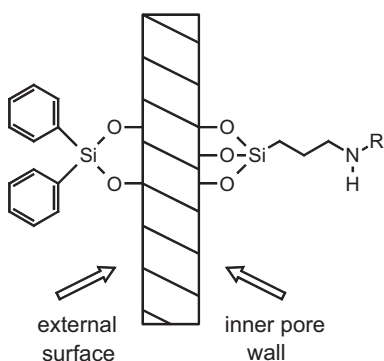
Structures of dyes discussed in the text.



methacrylate optical homogeneity was achieved.<sup>[15]</sup>

## Binding of Dye Molecules at Internal Pore Walls of Si-MCM-41

One possibility to overcome the leaching of chromophores and metal complexes from wide-porous materials is their covalent anchorage by a chemical reaction at pore walls of a molecular sieve. Covalent binding of functional molecules is useful for mesoporous M41S exhibiting in the case of Si-MCM-41 a pore diameter of  $\sim 3.1$  nm. Binding on the external surface cannot be excluded. Therefore after *method 1* in a first step the external surface of calcined and detergent free MCMs through the reaction with dichlorodiphenylsilane in THF at RT can be passivated.<sup>[16]</sup> Then in a second step aminopropyl-groups are introduced to the inner pore walls by the reaction of internal Si-OH groups with 3-aminopropyltriethoxysilane in dichloromethane at RT. In a third step the 3-aminopropylsilyl-MCM-41 is reacted with the sulfochloride of a phthalocyanine metal complex **3**, the sulfochloride of a sulfo-rhodamine B22 **4** (Figure 8) or a carboxylated azo dye either in dichloromethane, acetonitrile or DMSO to achieve covalent binding of the chromo-



**R = Bound to 3 (tetrasulfophthalocyanine) or 4 (sulfo-rhodamine B22)**

**Figure 8.**

Covalent grafting of dye molecules at internal pore walls of Si-MCM-41.

phores. Loadings with dyes of  $\sim 0.01$  mmol g<sup>-1</sup> were determined. If the silylation in the 2<sup>nd</sup> step is carried out with N-trimethoxysilylpropyl-N,N,N-trimethylammonium chloride positively charged internal walls are obtained.<sup>[16]</sup> Then with the negatively charged 2,9,16,23-tetrasulfophthalocyanine **3** in DMSO an ionic binding with loadings of  $\sim 0.1$  mmol g<sup>-1</sup> is achieved. The reflectance spectra in Figure 9 show by the characteristic Q band transition at  $\sim 670$  nm and indicate that the phthalocyanine metal complexes after covalent or ionic binding are mainly monomeric distributed in the internal walls of Si-MCM-41. Another possibility is the more simple impregnation of pore walls of Ti containing Si-MCM-41 with phthalocyanine metal complexes.<sup>[17]</sup>

Another method for covalent anchoring of chromophores at the walls of molecular sieves was recently developed. The idea is that after *method 2* one monomer for the hydrothermal synthesis contains a chromophore covalently bonded to one of the building blocks of the host lattice.<sup>[9]</sup> By co-condensation a covalent anchorage in the molecular sieve is achieved. In order to avoid splitting of the monomer-chromophore bond during crystallization, the microwave-assisted synthesis is advantageous. For the anchoring of dyes at Si-

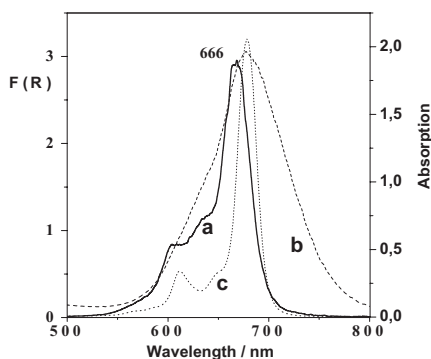


**Figure 9.**

Diffuse reflectance UV/Vis spectra of tetrasulfophthalocyanines in Si-MCM-41: (a) **3** (M=Si(IV)) ionically bound, (b) **3** (M=Zn(II)) covalently bound. (c) **3** (M=Zn(II)) in water in the presence of CTAC for comparison.

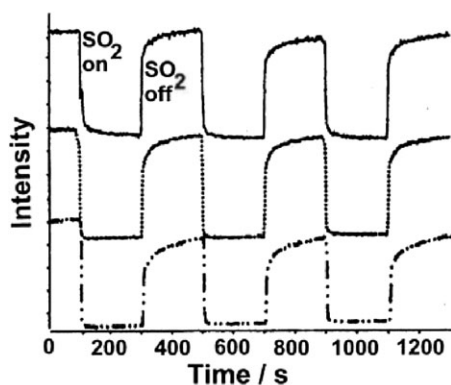


**Figure 10.**

Time dependence of the fluorescence intensity of **4** covalently bound at Si-MCM-41 in the presence and absence of  $\text{SO}_2$ . Middle and lower curve: **4** bound after method 2 or method 1, respectively; no detergent present. Upper curve: **4** bound after method 2; detergent present.

MCM-41 different dyes like the sulforhodamine B22 **4** were at first bonded to 3-aminopropyltriethoxysilane. A mixture of 2.4 g tetraethoxysilane and 6–125 mg modified dye were employed with cetyltrimethylammonium bromide in the synthesis of Si-MCM-41 which is finished under microwave conditions at 30 min. at  $130^\circ\text{C}$ . The template was removed then with aqueous HCl. The dye is monomolecular encapsulated.<sup>[9]</sup> The Rh B-Si-MCM-41 is highly fluorescent. Rhodamine dyes had been described as  $\text{SO}_2$  sensors due to the quenching of the fluorescence by this molecule.<sup>[18]</sup>

The open pore system of the host allows diffusion of molecules, especially gaseous ones. Interaction with guest molecules can alter the optical properties as known for specific optical sensors.<sup>[19]</sup> For better practical use the powdered samples can be dispersed in a polymer matrix. Sulforhodamine B22 **4** anchored at the walls of Si-MCM-41 was tested in a  $10\ \mu\text{m}$  thick film of a polysiloxane on glass as sensor. A very quick quenching of the fluorescence of the rhodamine dye bound at MCM and embedded in the polymer by  $\text{SO}_2$  when switching between the gases  $\text{N}_2$  and  $\text{SO}_2$  is observed (Figure 10).<sup>[20]</sup> The quenching

rate is determined by the diffusion of  $\text{SO}_2$  within the pores. In the as-synthesized sample containing the detergent the diffusion of  $\text{SO}_2$  is hindered (upper curve in Figure 10). The decrease of the fluorescence intensity is three times slower in comparison to two samples without detergent prepared after the two different before discussed procedures (middle and lower curves in Figure 10).

### Encapsulation of Dyes during the Hydrothermal Synthesis of Molecular Sieves

If dye molecules are added to the gel mixture of the hydrothermal molecular sieve synthesis, a co-inclusion (in addition to water and template) can occur. This method allows to encapsulate dye molecules exceeding the pore openings which means leaching-stable encapsulation. In order to achieve a successful formation of the lattice structure of the molecular sieve around dye molecules some pre-supposition must be fulfilled: The dye should be soluble in the gel mixture; alkaline or acidic pH, high reaction temperatures and long reaction times for the conventional molecular sieve synthesis can decompose the dye, therefore the microwave-assisted synthesis as discussed before is advantageous; if the diameter of the dye molecules exceeds the diameter of the internal void structure, they are included in mesopores surrounded by the crystalline lattice; care must be taken for the influence of the dye on phase purity and morphology. Encapsulation of various dyes in the framework of different molecular sieves were studied by us (exemplarily selected references): methylene blue in zeolites and  $\text{AlPO}_4$ ,<sup>[21a]</sup> thioindigo in zeolite faujasites,<sup>[21b]</sup> coumarin, rhodamine, oxazine dyes in  $\text{AlPO}_4$ -5,<sup>[7,22]</sup> phthalocyanine metal complexes in  $\text{AlPO}_4$ -5 and Si-MCM-41, and porphyrins in faujasites.<sup>[23]</sup>

Exemplarily, the addition of rhodamines in  $\text{AlPO}_4$ -5 (channel diameter 0.73 nm) is mentioned. A very suitable rhodamine dye

is rhodamine BE50 **5** (size  $\sim 0.85 \times 1.6 \text{ nm}^2$ ) which contains in the ester group a ternary amine comparable with the template tri-*n*-propylamine ( $\text{Pr}_3$ ).<sup>[7b]</sup> The total composition of the gel mixture employed for microwave-assisted crystallisation is 2.0  $\text{Pr}_3\text{N}$ : 1.0  $\text{Al}_2\text{O}_3$ : 1.0  $\text{P}_2\text{O}_5$ : 150  $\text{H}_2\text{O}$ : 0.0016–0.162 Rh dye. All synthesis batches produced after 45 min at  $T \sim 150^\circ\text{C}$  intensively fluorescent pink-colored Rh-loaded  $\text{AlPO}_4\text{-5}$  (color deepens with increase of dye uptake) of good crystallinity. The extent of encapsulation approaches a final limit of  $\sim 0.03$  expressed as the fraction dye molecules per unit cell which corresponds to around  $10^{-5} \text{ mol g}^{-1}$ . In the UV/vis reflectance spectra the position of the longest wavelength absorption at  $\sim 555\text{--}560 \text{ nm}$  is unchanged compared to aqueous solution. The intensity increases with higher loading. Important are the fluorescence spectra. The fluorescence intensities of the fluorescence bands at  $\lambda = 570\text{--}600 \text{ nm}$  depend on the dye loading and pass through a maximum at loadings of  $\sim 400$  to 200 unit cells (u.c.) per dye molecule. The dye concentration has been converted into average distances of the dye molecules. For an average chromophore distance of  $\sim 10\text{--}12 \text{ nm}$  highest fluorescence intensities of rhodamines are obtained which is shown in Figure 11 for different rhodamine dyes.

Now the fluorescent dyes coumarin 40 (**1**; size  $1.5 \times 0.6 \text{ nm}^2$ ), rhodamine BE50 (**5**; size  $1.6 \times 1.3 \text{ nm}^2$ ) and oxazine 1 (**6**,  $1.6 \times 0.85 \text{ nm}^2$ ) were successfully incorporated in one step during the microwave-assisted hydrothermal synthesis of  $\text{AlPO}_4\text{-5}$ .<sup>[22]</sup> It was found that the matching between the diameter of the  $\text{AlPO}_4\text{-5}$  channels and the dimensions of the dye molecules and also the solubility of the chromophores can result in distinct non-uniform distributions of the monomolecular encapsulated guest molecules. The incorporation of different dye molecules, absorbing and emitting light at different energies (Figure 12), enables a good panchromatic uptake of light, i.e., a light harvesting over a broad region of visible light. The energy of the entirely fixed dye molecules is transferred in a predominantly radiative mechanism from the dye absorbing at shorter wavelengths (coumarin 40) to the dye absorbing at higher wavelengths (oxazine 1) via a dye absorbing at intermediate wavelengths (rhodamine BE50). This is shown by exciting coumarin at short wavelengths and detecting the fluorescence of oxazine (Figure 13). The predominant energy transfer mechanism is radiative as concluded from the fluorescence decay analysis.

Recently, the orientation and dynamics of single dye molecules incorporated in the

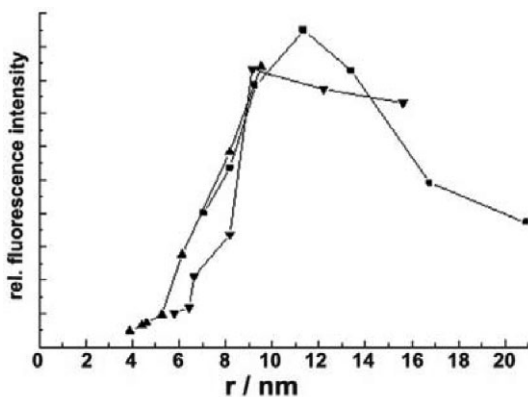


**Figure 11.**

Relative fluorescence intensity against the average separation of rhodamine dyes in  $\text{AlPO}_4\text{-5}$  (▲: rhodamine BE50 **5**; ■ rhodamine B; ▼: rhodamine 3B).<sup>[7b]</sup>



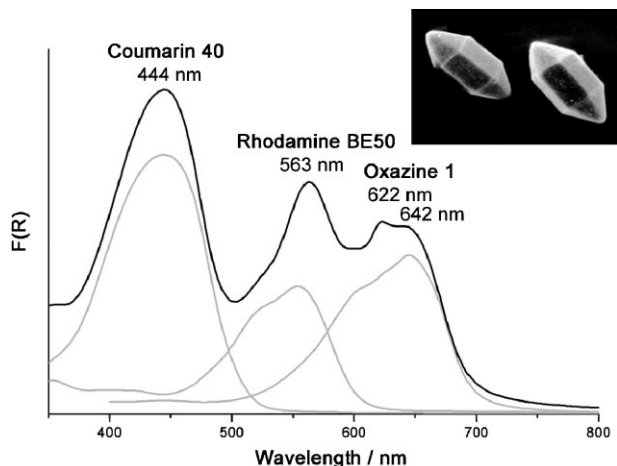


**Figure 12.**

Linear dependence of the absorption intensity in the diffuse reflectance spectra of  $\text{AlPO}_4\text{-5}$  loaded with a mixture of **1** (coumarin 40), **5** (rhodamine BE50) and **6** (oxazine 1) and of reference samples containing only one of the chromophores. Inset: Pencil-like hexagonal  $\text{AlPO}_4\text{-5}$  single crystals containing the dyes.

channels of the microporous and mesoporous materials were investigated in detail.<sup>[24]</sup> Single molecule spectroscopy is a modern and powerful tool that allows studying the interactions between an individual molecule and its immediate environment. The experimental data reveal the behaviour of each molecule directly. Oxazine 1 (**6**) dye

molecules were incorporated into the channels of microporous  $\text{AlPO}_4\text{-5}$  crystals in very low concentration which allows to look for single molecules. As shown in Figure 14a individual molecules are visible as individual fluorescence spots. Now, during the excitation the polarization is rotated continuously. The curves in

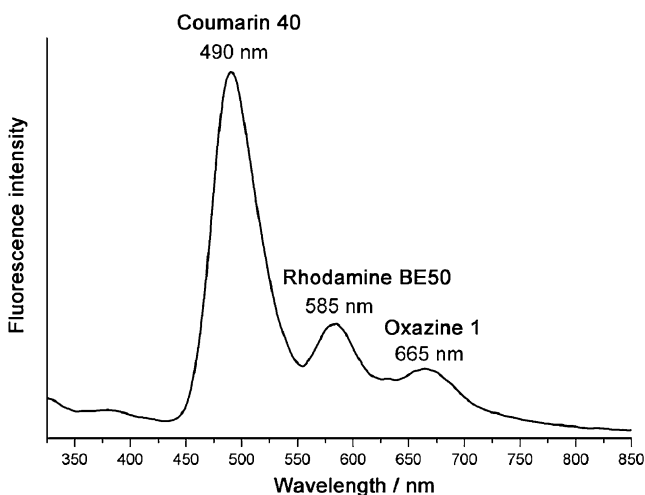


**Figure 13.**

Linear dependence of the fluorescence intensity in the fluorescence spectrum of  $\text{AlPO}_4\text{-5}$  loaded with the mixture of coumarin 40, rhodamine BE50 and oxazine 1 using an excitation at 300 nm.

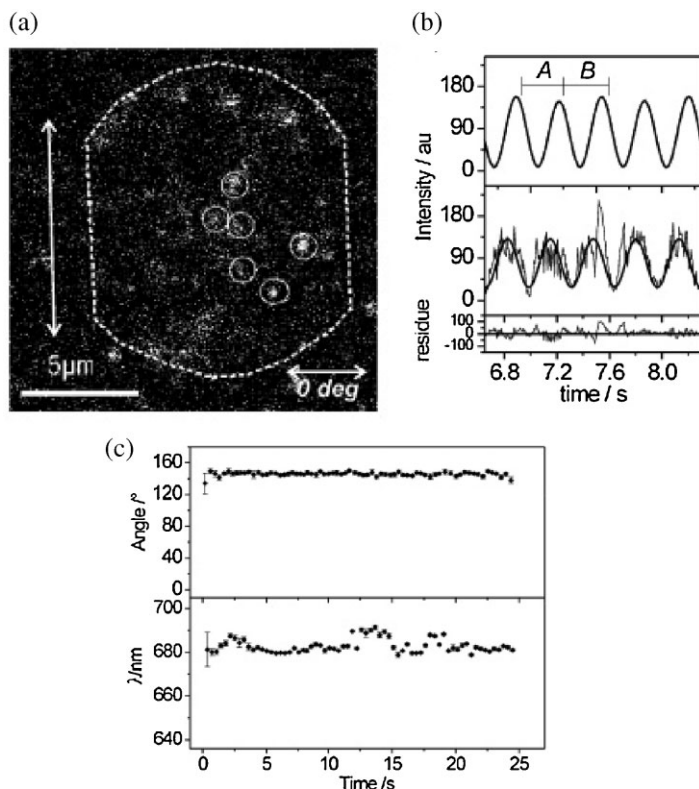


**Figure 14.**

Measurements of orientation and spectra of single molecules of oxazine 1 (**6**) in  $\text{AlPO}_4\text{-5}$  in low loadings of  $<10^{-10} \text{ mol g}^{-1}$ . (a) Confocal cross section through an  $\text{AlPO}_4\text{-5}$  crystal showing single molecules as diffraction-limited fluorescence spots. (b) Polarization-dependent intensity traces for transmitted excitation light (upper graph) and single-molecule fluorescence (lower graph). (c) Angular and spectral trajectories for an oxazine 1 molecule showing the most common case encountered in this system.

Figure 14b show the typical cosine-square modulation for the transmitted light (upper graph), and a single oxazine 1 molecule (lower graph). The orientation of the molecule remains constant with a value of  $\sim 143^\circ$ . The angular distribution of all molecules is broad and roughly aligned with the main axis of the crystal. Molecules remained with a fixed orientation during the measurement. This confirms the expectation that the tight fit of oxazine 1 molecules in  $\text{AlPO}_4\text{-5}$  results mainly in immobile molecules that do not have any freedom to move or to rotate. The data analysis of the modulated intensity trace and sequence of spectra gives  $\Phi(t)$ , the angular trajectory, and  $\lambda_m(t)$ , the spectral trajectory. The graphs in Figure 14c show

the corresponding data for the molecule displaying a more representative oxazine-1 molecule in an  $\text{AlPO}_4\text{-5}$  crystal. The orientation of the molecule also remains constant ( $149 \pm 5^\circ$ ) while the spectra fluctuate rapidly only around a mean value of 685 nm in a range of 2 to 8 nm. Therefore oxazine-1 in  $\text{AlPO}_4\text{-5}$  do not have the freedom to re-orient and show limited spectral dynamics. This system represents a static material in which the molecules are entrapped and immobilized in a solid matrix and stands as an example for a static host-guest material, which is desirable for solid-state optical applications. As second host-guest system the movement of a terrylenediimide dye molecules inside the mesoporous network of Si-MCM-41

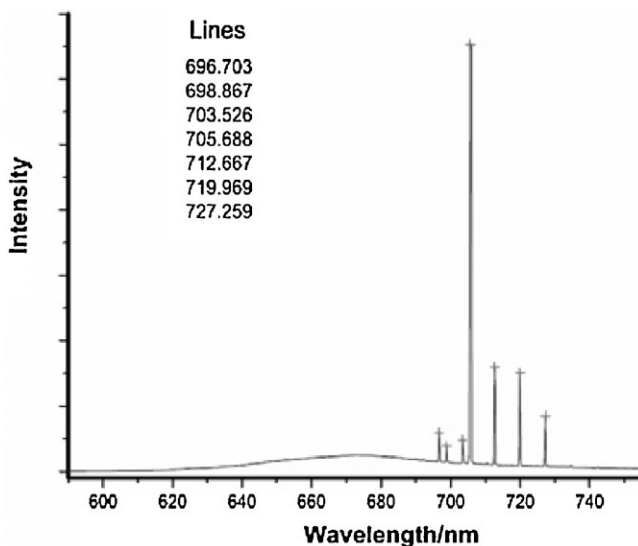


**Figure 15.**

Lasing spectrum of an oxazine 1 loaded  $\text{AlPO}_4\text{-5}$  microcrystal with a concentration around 75 unit cells per dye molecule and size of 7.5  $\mu\text{m}$  width over flats.

was studied.<sup>[24b]</sup> This type of system stands as an example for materials in which dynamics play a fundamental role, as is desirable for sensor and catalysis applications.

After detailed analysis of fluorescence behaviour of different laser dyes in  $\text{AlPO}_4\text{-5}$  the lasing properties were investigated.<sup>[2,25]</sup> For example,  $\text{AlPO}_4\text{-5}$  crystals with a barrel-shaped morphology in a length of  $\sim 8 \mu\text{m}$  (see Figure 2a) in the crystallographic *c*-axis containing rhodamine BE50 (**5**) or oxazine 1 (**6**) (content  $\sim 0.5 \text{ wt-\%}$ ,  $\sim 75$  dye molecules per unit cell) were selected. The microcrystals were pumped with 10 ns pulses from the 532 nm second harmonic of a Nd:YAG-laser delivered to the sample with an optical fibre. Stimulated emission was observed to occur on several sharp lines with instrument resolution limited width (Figure 15). The emission is concentrated along the crystal edges. The complex emission distribution is compatible with the simultaneously recorded spectrum which reveals multi-mode emission. The properties of resulting microlasers depend on size and shape of the microresonators, which was discussed as

model for microscopic hexagonal ring resonators. In a dielectric hexagonal prism light rays can be confined by repeated internal reflection to form a ring resonator, and the resulting light distribution circulates around as a whispering-gallery mode. Photostability as important parameter was also studied.

## Conclusion

Polycondensations of oxygen containing tetrahedra of the metal aluminium, the semimetal silicon and the non-metal phosphorus in the presence of structure directing agent results in microporous and mesoporous molecular sieves like zeolite faujasites,  $\text{AlPO}_4\text{-5}$  and Si-MCM-41. The microwave-assisted hydrothermal synthesis is advantageous compared to the conventional procedure due to the short reaction time. But care must be taken to get the right phase and suitable morphologies. Permanent encapsulation of various dyes after different methods was achieved: *in-situ* synthesis in the framework of faujasites, binding at internal pore walls if mesoporous

molecular sieves, addition to the hydrothermal mixture of the synthesis mixture. Monomolecular distribution of dyes in the framework of the hosts is obtained. After single molecule spectroscopy dye molecules in AlPO<sub>4</sub>-5 show a distinct and stable orientation along the channel axis. The molecules in this medium act as reporter on a distinct orientation. The high absorption and fluorescence intensities of the encapsulated dyes show their monomolecular distribution in the framework of the hosts. Based on these findings the composite materials are interesting for optical applications. This was successfully shown for photochromic switches, optical sensors and lasing.

- [1] [1a] G. A. Ozin, A. Kuperman, A. Stein, *Angew. Chem., Int. Ed. Engl.* **1989**, 28, 359; [1b] M. E. Davis, *Nature* **2002**, 417(6891), 813; [1c] G. Wirnsberger, G. D. Stucky, *Chem. Phys. Chem.* **2000**, 1, 90.
- [2] F. Laeri, F. Schüth, U. Simon, M. Wark, Eds., “Host-Guest-Systems Based on Nanoporous Crystals”, WILEY-VCH, Weinheim **2003**.
- [3] G. Schulz-Ekloff, D. Wöhrle, R. A. Schoneydt, *Microporous Mesoporous Mater.* **2002**, 51, 91.
- [4] [4a] A. Dyer, “An Introduction to Zeolite Molecular Sieves”, J. Wiley & Sons, New York **1988**; [4b] D. W. Breck, “Zeolite Molecular Sieves – Structure, Chemistry and Use”, J. Wiley & Sons, New York **1974**.
- [5] [5a] S. T. Wilson, B. M. Lok, C. A. Messina, T. R. Cannan, E. M. Flanigen, *J. Amer. Chem. Soc.* **1982**, 104, 1146; [5b] S. T. Wilson, “Introduction to Zeolites and Science and Practice”, Amsterdam **1991**.
- [6] [6a] C. T. Kresge, M. E. Leonowicz, W. J. Roth, J. C. Vartuli, J. S. Beck, *Nature* **1992**, 359, 710; [6b] F. Hoffmann, M. Cornelius, J. Morell, M. Fröba, *Angew. Chem.* **2006**, 118, 3290.
- [7] [7a] I. Braun, G. Schulz-Ekloff, M. Bockstette, D. Wöhrle, *Zeolites* **1997**, 19, 128; [7b] M. Bockstette, D. Wöhrle, I. Braun, G. Schulz-Ekloff, *Microporous Mesoporous Mater.* **1998**, 23, 83; [7c] M. Ganschow, G. Schulz-Ekloff, M. Wark, M. Wendschuh-Josties, *J. Mater. Chem.* **2001**, 11, 1823.
- [8] [8a] S. Oliver, A. Kuperman, G. A. Ozin, *Angew. Chem.* **1998**, 110, 49; [8b] S. Oliver, A. Kuperman, A. Lough, G. A. Ozin, *Chem. Mater.* **1996**, 8, 2391.
- [9] M. Ganschow, M. Wark, D. Wöhrle, G. Schulz-Ekloff, *Angew. Chem Int. Ed. Engl.* **2000**, 39, 161.
- [10] C. Y. Chen, H.-X. L. Li, M. E. Davis, *Microporous Mater.* **1993**, 2(17), 27.
- [11] G. Meyer, D. Wöhrle, M. Mohl, G. Schulz-Ekloff, *Zeolites* **1984**, 4, 30.
- [12] C. Schomburg, D. Wöhrle, G. Schulz-Ekloff, *Zeolites* **1996**, 17, 232.
- [13] C. Schomburg, M. Wark, Y. Rohlfing, G. Schulz-Ekloff, D. Wöhrle, *J. Mater. Chem.* **2001**, 11, 2014.
- [14] [14a] J. R. Crano, R. J. Guglielmetti, “Organic Photochromic and Thermochemical Compounds”, Vol. 2, Kluwer/Plenum, New York **1999**; [14b] H. Dürr, H. Bonas-Laurent, Eds., “Photochromism”, Elsevier, Amsterdam **1990**.
- [15] J. Schneider, D. Fanter, M. Bauer, C. Schomburg, D. Wöhrle, G. Schulz-Ekloff, *Microporous Mesoporous Mater.* **2000**, 39, 257.
- [16] [16a] Y. Rohlfing, D. Wöhrle, J. Rathousky, A. Zukal, M. Wark, *Studies in Surface Science and Catalysis*, **2002**, 142, 1067
- [16b] Y. Rohlfing, *Dissertation*, University Bremen. **2004**.
- [17] [17a] A. Ortlam, M. Wark, G. Schulz-Ekloff, J. Rathousky, A. Zukal, *Mesoporous Molecular Sieves, Studies in Surface Science and Catalysis* **1998**, 117, 357; [17b] M. Wark, A. Ortlam, M. Ganschow, G. Schulz-Ekloff, D. Wöhrle, *Ber. Bunsenges. Phys. Chem.* **1998**, 102, 1548.
- [18] A. Sharma, O. S. Wolfbeis, *Spectrochem. Acta* **1987**, 43A, 1417.
- [19] [19a] B. D. MacCraith, *Chem. Anal.* **1998**, 150, 195; [19b] O. S. Wolfbeis, “Fiber Optic Chemical Sensors and Biosensors”, CRC Press, Boca Raton **1991**.
- [20] M. Wark, G. Grubert, M. Warnken, G. Schulz-Ekloff, M. Ganschow, Y. Rohlfing, T. Bogdahn-Rai, D. Wöhrle, in: “Applied Mineralogy”, Rammimair et al. ed., Balkema, Rotterdam **2000**, p. 253 ff.
- [21] [21a] R. Hoppe, G. Schulz-Ekloff, D. Wöhrle, C. Kirschhock, H. Fuess, R. Schoneydt, *Adv. Mater.* **1995**, 7, 61; [21b] R. Hoppe, G. Schulz-Ekloff, D. Wöhrle, C. Kirschhock, H. Fuess, *Langmuir* **1994**, 10, 1517.
- [22] M. Ganschow, C. Hellriegel, E. Kneuper, M. Wark, C. Thiel, G. Schulz-Ekloff, C. Bräuchle, D. Wöhrle, *Adv. Funct. Mater.* **2004**, 14, 269.
- [23] [23a] D. Wöhrle, A. Sobbi, O. Franke, G. Schulz-Ekloff, *Zeolites* **1996**, 15, 293; [23b] M. Ganschow, D. Wöhrle, G. Schulz-Ekloff, *J. Porphyrins Phthalocyanines* **1999**, 3, 299; [23c] C. Thiel, *Dissertation*, University Bremen, **2005**.
- [24] [24a] C. Seebacher, C. Hellriegel, C. Bräuchle, M. Ganschow, D. Wöhrle, *J. Phys. Chem. B* **2003**, 107, 5445; [24b] C. Jung, C. Hellriegel, B. Platscheck, D. Wöhrle, T. Bein, J. Michaelis, C. Bräuchle, *J. Am. Chem. Soc.* **2007**, in press.
- [25] I. Braun, G. Ihlein, F. Laeri, J. U. Nöckel, G. Schulz-Ekloff, F. Schüth, U. Vietze, O. Weiß, D. Wöhrle, *Appl. Phys. B* **2000**, 70, 335.